Measurement 260 (2026) 119795

Contents lists available at ScienceDirect

Measurement

journal homepage: www.elsevier.com/locate/measurement

Field evaluation of four state-of-the-art astrogeodetic systems along the Mississippi River: CODIAC, VESTA, QDaedalus and TSACS

Müge Albayrak [a,*], Ryan A. Hardy [b], Benjamin A. Fernandez [c], Jon Cliburn [c], Aline P. Baeriswyl [d], Daniel Willi [e], Sébastien Guillaume [d]

[a] School of Civil and Construction Engineering, Oregon State University, Corvallis, OR 97331, USA
[b] NOAA National Geodetic Survey, Boulder, CO 80305, USA
[c] Louisiana Spatial Reference Center, Louisiana State University, LA 70803, USA
[d] School of Management and Engineering Vaud (HEIG-VD), University of Applied Sciences and Arts Western Switzerland (HES-SO), 1400 Yverdon-les-Bains, Switzerland
[e] Federal Office of Topography swisstopo, 3084 Bern, Switzerland

ARTICLE INFO

Keywords:
Deflections of the vertical
Geodetic astronomy
Zenith camera
Robotic total station
CODIAC
VESTA
QDaedalus
TSACS

ABSTRACT

Deflections of the vertical, which quantify the direction of gravity near the Earth's surface, are conventionally observed using astrogeodetic instruments. Our research compared four astrogeodetic systems together for the first time at similar observing sites: the zenith cameras COmpact DIgital Astrometric Camera (CODIAC) and VErtical by STArs (VESTA), and the robotic total station-based astrogeodetic systems QDaedalus and Total Station Astrogeodetic Control System (TSACS). We deployed the four systems at 32 sites on a 190 km profile along the Mississippi River between Baton Rouge and New Orleans, using 14 primary sites for direct comparison and subsequent performance evaluation with analysis of variance (ANOVA) and least-squares bias analysis. The results demonstrate that CODIAC is able to have an internal consistency better than ± 0.05 arcseconds for its 20-minute observations. Relative to CODIAC, the results suggest that, for 45-minute occupations in a typical astrogeodetic campaign, the VESTA, QDaedalus, and TSACS are capable of 0.15–0.20 arcsecond accuracy. One of the main goals of the survey was to fill gaps in geoid validation data in this region; these results will be used to test the National Geodetic Survey's new GEOID2022 model and design future field campaigns. This survey also highlights the challenges of designing an astrogeodetic profile in a busy commercial corridor and serves as an instructive experience in 21st century operational geodetic astronomy.

1. Introduction

Deflections of the vertical (DoV) are conventionally measured using specially developed astrogeodetic instruments to quantify the direction of gravity near the Earth's surface. These instruments use telescopes and precisely timed image sensors to measure the directions of stars relative to the local plumb line, which is established by a dynamically free instrument component such as a fluid or pendulum. These measurements of star directions relative to the plumb line can be combined to estimate the astronomical coordinates (astronomical latitude Φ and longitude Λ), which describe the direction of the plumb line in a global Earth-fixed reference frame. Subtracting geodetic coordinates (geodetic latitude φ

Abbreviations: **ACSYS2**, Astrogeodetic Camera SYStem 2; **ANOVA**, Analysis of Variance; **CCD**, Charge-Coupled Device; **CHGeo2004**, Swiss geoid model 2004; **CMOS**, Complementary Metal-Oxide Semiconductor; **CODIAC**, COmpact DIgital Astrometric Camera; **CPRA**, Coastal Protection ansd Restoration Authority; **C4G**, Center for Geoinformatics; **C4GNET**, Center for Geoinformatics Network; **DIADEM**, Digital Astronomical Deflection Measuring System; **DoV**, Deflections of the Vertical; **EGM2008**, Earth Gravitational Model 2008; **ETH**, Eidgenössische Technische Hochschule; **FK6**, Sixth Catalogue of Fundamental Stars; **GAIA EDR3**, Gaia Early Data Release 3; **GeMS**, Geoid Monitoring Service; **GGMplus**, Global Gravity Model plus; **GNSS**, Global Navigation Satellite System; **GSVS**, Geoid Slope Validation Survey; **ITRF**, International Terrestrial Reference Frame; **ITRS**, International Terrestrial Reference System; **LSU**, Louisiana State University; **NAVD 88**, North American Vertical Datum of 1988; **NGS**, National Geodetic Survey; **NOAA**, National Oceanic and Atmospheric Administration; **OSU**, Oregon State University; **RTK**, Real-Time Kinematic; **TSACS**, Total Station Astrogeodetic Control System; **TZK2-D**, Transportable Zenith Camera 2-Digital; **UCAC4**, Fourth U.S. Naval Observatory CCD Astrograph Catalogue; **VESTA**, VErtical by STArs; **UTC**, Coordinated Universal Time.

* Corresponding author.
E-mail addresses: muge.albayrak@oregonstate.edu (M. Albayrak), ryan.hardy@noaa.gov (R.A. Hardy), bferna4@lsu.edu (B.A. Fernandez), jclibu1@lsu.edu (J. Cliburn), aline.pauline.baeriswyl@gmail.com (A.P. Baeriswyl), daniel.willi@swisstopo.ch (D. Willi), sebastien.guillaume@heig-vd.ch (S. Guillaume).

https://doi.org/10.1016/j.measurement.2025.119795
Received 28 September 2025; Received in revised form 3 November 2025; Accepted 18 November 2025
Available online 21 November 2025

and longitude λ) from these astronomical coordinates is the first step to computing the DoV [1,2]. DoV has two broad categories of practical use cases: orienting terrestrial survey and navigation data to a global reference frame and quantifying the slope of the geoid. The latter use case is especially important for defining geopotential datums and height systems as closely spaced measurements of the DoV may be used to profile the geoid (e.g., [3]).

While the core principle of measuring DoV is ancient, the state-of-the-art in astrogeodetic systems is represented by only a small number of systems developed worldwide. Recent decades have seen the development of operational astrogeodetic systems in Switzerland [4,5], Latvia [6], China [7,8], the USA [9,10] and Russia [11]. Researchers in each of these countries have developed zenith cameras, while Switzerland, China, and the USA have also developed systems based around commercially available robotic total stations. Additionally, another total station-based system was developed at the Astronomical Institute of the Romanian Academy in Romania [12]. For this research, we compared four astrogeodetic systems at colocated field observation sites in the U.S. state of Louisiana. These included two zenith cameras, the COmpact DIgital Astrometric Camera (CODIAC), developed at Eidgenössische Technische Hochschule (ETH) Zurich in Switzerland, and VErtical by STArs (VESTA), developed at the University of Latvia, and two robotic total station-based astrogeodetic systems, the QDaedalus, also developed at ETH Zurich, and the Total Station Astrogeodetic Control System (TSACS), developed by National Oceanic and Atmospheric Administration's (NOAA) National Geodetic Survey (NGS) in the USA.

There are only a few studies comparing the performance of astrogeodetic systems due to the limited number of active systems. Hirt et al. [13] compared the previous version of CODIAC, the Digital Astronomical Deflection Measuring System (DIADEM) [14], with the Transportable Zenith Camera 2-Digital (TZK2-D), which was developed at the University of Hannover [15,16], at different sites in Switzerland in 2003 and 2005. This comparison was conducted through simultaneous parallel measurements. Hauk et al. [17] compared data collected by the TZK2-D from 2006 to 2010 [18] with QDaedalus data from 2016 at six benchmarks in the Bavarian Alps to assess the latter's accuracy, while Albayrak et al. [19] performed a similar comparison at ten benchmarks in the Munich region in 2018. Albayrak et al. [20] determined the accuracy of Astrogeodetic Camera SYStem 2 (ACSYS2) in Türkiye using QDaedalus in Istanbul through repeated observations at the same benchmark in 2018. Hardy et al. [21] compared CODIAC data collected in Virginia in 2014 with TSACS reoccupations conducted in 2021. More recently, Albayrak et al. [22] compared CODIAC with QDaedalus, and Varna et al. [23] compared CODIAC with VESTA using simultaneous parallel measurements in Switzerland over several nights in 2021. This study represents the first instance in which four different astrogeodetic systems were deployed together for a field comparison along a profile.

The CODIAC, VESTA, QDaedalus and TSACS systems used in this research employ different observation techniques and data processing strategies. The fundamental distinction is between zenith cameras and total stations. Zenith cameras use large (~200 mm) telescopes to observe groups of faint stars within a degree of the zenith. Total stations are used in the same manner as historical geodetic astrolabes and observe the elevation angles of individual bright stars near a consistent elevation angle (60 degrees) over a wide range of azimuths. These elevation angles may be used to recover the DoV using least-squares [24]. While the CODIAC and VESTA cameras share standard zenith camera components (telescope, image sensors such as charge-coupled device (CCD) or complementary metal-oxide semiconductor (CMOS), tiltmeters, GPS receiver and antenna, laptop, and substructure—none of which are identical across the two systems), several of the main components of the QDaedalus and TSACS systems differ significantly. For instance, the QDaedalus incorporates many components, such as a robotic total station, external CCD camera, meniscus lens, interface box for time synchronization, Global Navigation Satelite System (GNSS) receiver and antenna, and external 12 V battery. In contrast, TSACS, which utilizes the total station's internal CMOS camera, includes only a control module consisting of a microcontroller, GPS module, pressure/temperature sensor to command the total station, and a Raspberry Pi single-board computer to record the data. The DoV data collected using these systems and CODIAC's earlier versions have been utilized for many different purposes, such as determining the national geoid model in Switzerland (Swiss geoid model 2004 *CHGeo2004* [25]) and the quasi-geoid model of Latvia [26], conducting Geoid Slope Validation Surveys (GSVSs) in Texas, Iowa and Colorado in the USA [[27,28,29]], validating global gravity field models (e.g., Global Gravity Model plus *GGMplus* [30] and the Earth Gravitational Model 2008 *EGM2008* [31]) in Istanbul, Türkiye [19], and the Geoid Monitoring Service (GeMS) validation survey in Alaska, USA [32], among others.

To assess the performance of multiple astrogeodetic systems, our research team deployed four astrogeodetic systems along a profile consisting of 32 sites spanning approximately 190 km along the Mississippi River between Baton Rouge and New Orleans. The main goal of this survey was to directly compare the four instruments to obtain insights into instrument performance. A second goal was geoid validation, which is not addressed in this paper, but was important for the design of the profile. All four of these systems were deployed on 14 of these sites. To densify this profile to 5 km spacing for geoid determination, an additional 18 secondary observing sites were occupied using VESTA with either CODIAC or QDaedalus.

The selected segment of the Mississippi River has an especially urgent need for accurate orthometric heights to predict water flow, as it is the USA's most intensive commercial corridor by freight volume [33]. Orthometric heights are most commonly obtained using geodetic leveling. In the USA, the attrition of marks, systematic errors in North American Vertical Datum of 1988 (NAVD 88), and the high cost of new leveling make a leveling-based height system impractical in a modernized spatial reference system. The issue of accurate orthometric heights is expected to be addressed by the NGS's new geopotential datum, based on GEOID2022, a gravimetric geoid model with a nominal accuracy of 1 cm [34]. However, the construction, validation, and maintenance of this geoid model are challenging in Louisiana due to rapid subsidence. The Louisiana Coastal Protection and Restoration Authority (CPRA) provides guidance on subsidence rates, indicating a lower scenario of 2–6 mm/yr and a higher scenario of 2–8 mm/yr in our project area, while other areas further downriver experience even greater rates of ~ 10–25 mm/yr [35]. Such subsidence complicates the comparison of GNSS with leveling, the most fundamental method for validating geoid accuracy, and poses a significant challenge due to the lack of dense terrestrial gravity data required for geoid modeling. Given these limitations, geodetic astronomy presents a viable solution for geoid slope validation with minimal sensitivity to height errors. Astrogeodetic DoV could also help fill critical data gaps in the region, improving the accuracy of geoid-based height determinations.

The remainder of this paper is organized as follows. Section 2 describes the instrumentation and measurement methods used in this study, including the design and operation of the four astrogeodetic systems. Section 3 outlines the survey design along the Mississippi River and the criteria for site selection. Section 4 summarizes the field data collection procedures and the characteristics of the observed datasets. Section 5 presents the least-squares analyses used to estimate instrument biases and evaluate precision. Section 6 discusses the comparative performance of the instruments and interprets the results in terms of operational trade-offs. Finally, Section 7 provides conclusions and recommendations for future work in astrogeodetic system development and geoid validation.

2. Instrumentation and measurement methods

Our research team deployed two zenith cameras (CODIAC and VESTA) and two robotic total station-based systems (QDaedalus and

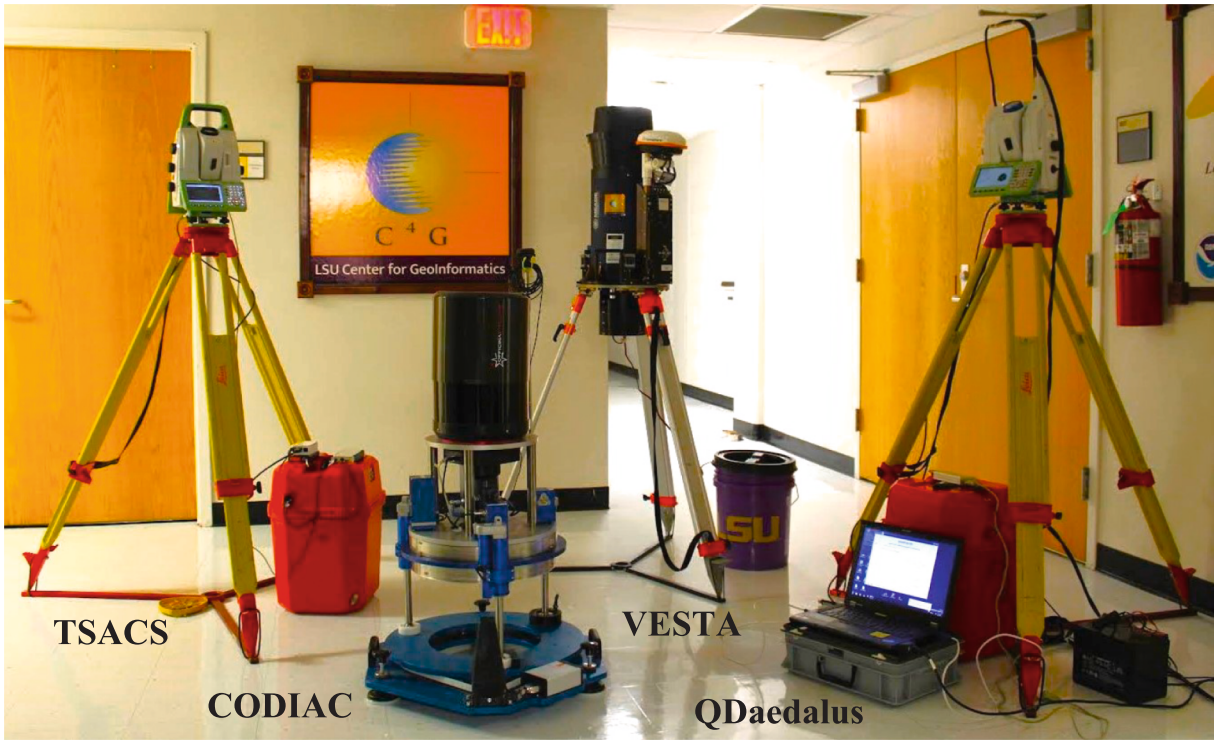

Fig. 1. TSACS, CODIAC, VESTA, and QDaedalus systems at the Center for Geoinformatics (C4G) at Louisiana State University (LSU).

TSACS) to observe DoVs along the Mississippi River. This campaign marked the first use of CODIAC following its CMOS camera upgrade in March 2024. Prior to this upgrade, CODIAC had been compared with QDaedalus [22] and VESTA [23] in Switzerland. We compared DoV data collected with CODIAC from before (2021) and after (2025) the CMOS upgrade at the Zimmerwald Observatory in Switzerland. The statistical results are presented in Table A1., which demonstrate that the N–S DoV component remains consistent before and after the CMOS upgrade. The E–W component also shows close agreement between the two periods. Importantly, the temperature-dependent drift observed during nighttime sessions before the upgrade is no longer present. TSACS, developed in 2020, has been employed in fieldwork since its introduction, and its details are published here for the first time. All four astrogeodetic systems are shown together in Fig. 1. Test measurements for each system were conducted at the Center for Geoinformatics (C4G) at Louisiana State University (LSU) before, during, and after the campaign.

2.1. Fundamental components of astrogeodetic systems

The four systems employ different approaches to astronomic position measurement. All astrogeodetic systems rely on three components to establish the direction of the plumb line in the global terrestrial reference frame:

1. A subsystem to measure the *angles of stars* relative to the instrument body (e.g., a telescope and an image sensor or micrometer)

All four systems measure the angles of stars by imaging them, but zenith cameras are distinguished from total stations by the choice of target stars. Zenith cameras image a narrow patch of sky and must have a larger telescope aperture and highly sensitive imaging sensors to capture a sufficient number of dim stars. Total stations have a smaller aperture and must individually image bright stars farther from the zenith. Dim stars are generally farther away and have less parallax and proper motion, ensuring stable celestial reference frame ties. In comparison, brighter stars have higher parallax and proper motion and thus require position data from mature catalogs with long observation spans. Another disadvantage of bright stars is subtle, but pronounced, biases in the centroid due to binary companions.

2. A subsystem to measure the *inclination of the instrument body* relative to the plumb line (e.g., a compensator, pendulum, tiltmeter, or natural water horizon)

The astrogeodetic systems in this study use only two inclination measurement techniques: high-precision tiltmeters (zenith cameras) and commercial-grade compensators built into the total stations [36]. Both systems, while sensitive, are subject to an unknown bias that may be removed by physically reversing the instrument and comparing with multiple celestial observations.

3. A subsystem for measuring *time* to relate the observed position of stars to the terrestrial reference frame (e.g., a clock referenced to Coordinated Universal time (UTC), plus Earth-orientation parameters) and the instrument's local geodetic horizontal frame

The third of these components is less challenging in the 21st century due to the proliferation of nanosecond time signals from GNSS and the routine measurement of Earth orientation parameters. All four systems use GNSS-based timing for their measurements. However, aligning these time signals with image exposures still presents a significant engineering challenge, which these systems solve in different ways.

2.2. Design and features of the instruments

The different approaches to addressing the challenges of measuring star angles, instrument inclination, and timing have resulted in markedly different system designs. The designs of the four instruments are shown in Fig. 2. These design choices result in tradeoffs between field operability and scientific utility. The best system choice depends on the fieldwork's specific requirements. Copies of TSACS, VESTA, and QDaedalus are owned by multiple institutions. Louisiana State

Fig. 2. Design features of (a) VESTA, (b) CODIAC, (c) TSACS, and (d) QDaedalus systems.

University (LSU) owns a VESTA. The Technical University of Munich [17], Budapest University of Technology [37], and Oregon State University (OSU) each own a QDaedalus system. The Ohio State University has built and deployed a TSACS with NGS guidance [38]. Although CODIAC has been used in NGS's GSVS surveys [[27,28,29]], its availability to NGS is otherwise limited. The Federal Office of Topography swisstopo currently operates CODIAC.

Since each astrogeodetic system is unique, its components and specifications are detailed in Table 1. Some specifications are common to all four systems, such as data processing—which is normally not performed in real time—and their high susceptibility to wind.

Other specifications vary based on the type of system:

Celestial measurements: Zenith cameras capture star images at the zenith, while total station-based systems image individual stars along the almucantar, a celestial small circle centered on the zenith. Zenith cameras image stars within less than one degree of the zenith and must have larger telescope apertures able to observe dimmer stars. Total station-based systems observe stars at a zenith angle of approximately 30 degrees, a conventionally selected angle that aims to maximize the availability of bright stars while keeping refraction error managably minimal. This angle is partially driven by the 30-degree reflection angles commonly found in equilateral prisms used by astrolabes throughout the 20th century. Astrolabes and total station-based systems use a fixed or nearly fixed zenith angle to keep refraction errors approximately constant.

Inclination measurement: Zenith cameras universally use pendulum-based Lippmann tiltmeters [45] for high-precision inclination measurements; CODIAC also employs redundant orthogonally mounted Wyler tiltmeters to confirm the Lippmann results. Total station-based

Table 1
The components and specifications of the CODIAC, VESTA, QDaedalus, and TSACS systems.

	Astrogeodetic Systems	CODIAC	VESTA	QDaedalus	TSACS
Components (name/ company)	Telescope	Riccardi-Honders Astrograph 200 mm f/3 (RH 200AT)/Officina Stellare	Meade LX-200/Meade Instruments 200 mm f/10	Leica TS60/Leica 50 mm f/ 4.6	Leica TS60/Leica 50 mm f/4.6
	CCD/CMOS camera	CMOS: SVS-Vistek exo342MU3 (since 2024)	CCD: SBIG STF-8300 M/ SBIG	CCD: Guppy F-080C /Allied Vision Technologies	CMOS: Micron/ MT9P031
	GPS receiver	NEO-M8/u-blox	Hemisphere A222/ Hemisphere GNSS	NEO-M8/u-blox	MTK3339
	Tiltmeter	2 HRTM/Lippmann + 2 Wyler/ Wyler	1 HRTM/Lippmann	Leica TS60/Leica	Leica TS60/Leica
	Focuser	FLI ATLAS/Finger Lakes Instrumentation	N/A	Leica TS60/Leica + Meniscus lens	Leica TS60/Leica
	Substructure	Specifically designed (fully automatic)	Tripod with custom disc on top	Industrial standard tripod	Industrial standard tripod
Specifications	Developer	ETH Zurich/Switzerland	University of Latvia/Latvia	ETH Zurich/Switzerland	NGS/USA
	Year of initial development	2014 [4]	2016 [6]	2014 [5]	2020 [10]
	Previous version	DIADEM [14]	N/A	ICARUS [39]	N/A
	Purpose of the system	Astrogeodetic measurements	Astrogeodetic mea.	Astrogeodetic & geodetic mea.	Astrogeodetic mea.
	Precision and accuracy	0.05″ [22]	0.1″ [40]	0.1″ [22]	0.2″ [21]
	Star catalogue	The fourth US naval observatory CCD astrograph catalogue (UCAC4) [41]	GAIA Early Data Release 3 (GAIA EDR3) [42]	Sixth Catalogue of Fundamental Stars (FK6) [43]	Hipparcos [44]
	Observable star magnitude	Up to ~ 16 magnitude (mag.)	Up to ~ 12–14 mag	Bright stars only (≤6 mag)	Bright stars only (≤6 mag)
	Laptop specifications	50 GB free memory required per night	No special requirement	Express card insertion required	Headless Raspberry Pi
	Remote control	Possible	Fully remote	N/A	Fully autonomous
	Weight of the system	120 kg.	20 kg.	20 kg.	20 kg.
	Duration of observations	10 min./series (2 series/session)	30–50 min./session	15 min./series (4 series/ session)	15 min./series (4 series/session)
	Data processing time	Lengthy data processing time	Lengthy data processing time	1 min.	1 min.
	Number of systems	2	4	6+	4
	Required operators	2	1	1	1
Operational and Logistical Factors*	Ease of construction	Difficult	Difficult	Easy	Easy
	Measurement speed	Highest	Moderate	Moderate	Moderate
	International shipping	Difficult	Moderate	Easy	Easy
	Cost of international campaign	Highest	Moderate	Moderate	Moderate
	Operator supervision	Moderate	Easy	Moderate	Easy
	Operator training time	Several hours	~1 h	~2 h	< 1 h

systems, on the other hand, use compensators, which are typically based on reflections of a coded image on a silicone-oil-free surface [36].

Rotation positions: All astrogeodetic systems must rotate to remove the bias in their inclination measurements. In general, a minimum of three unique rotation positions is required to separate inclination bias from DoV components. Zenith cameras have specific rotation positions. For instance, VESTA typically uses 20–32 rotation positions, and CODIAC uses four. In contrast, total station-based systems do not have fixed rotation positions and instead rotate their bodies to the azimuth of their target star.

Installation: Both classes of instrument can be transported to field sites and set up without any special infrastructure. However, the size and weight of some zenith cameras can restrict operators from operating on inclined surfaces or transporting the instrument far from a vehicle. A notable exception is VESTA, which is light enough to be carried by a single person. Total station-based systems can be installed on survey pillars using a standard thread, while zenith cameras cannot. None of the total stations were installed on pillars for this survey, but these are common features at geodetic observatories.

VESTA, QDaedalus, and TSACS have tripod substructures and are lightweight, whereas CODIAC's substructure is significantly heavier, and requires two operators to transport (see Table 1). Consequently, conducting CODIAC operations far from transportation infrastructure is challenging, which plays a critical role in selecting the observation sites. Certain specifications, such as installation time, are not included in Table 1 but are worth mentioning. CODIAC weighs 120 kg and requires transportation in two boxes via a commercial vehicle. Due to the weight of the boxes, carrying them to the benchmark can be challenging. However, once unpacked, the installation takes less than five minutes. Thus, while the installation process is quick, the overall required time depends on the distance to the benchmark and its accessibility. In comparison, TSACS and VESTA require less than five minutes for installation, while QDaedalus involves more hardware and cables to connect to the total station, inflating the installation time to at least five minutes. Based on our field experience in Louisiana, VESTA, QDaedalus, and TSACS each acquired 4–5 marks per fully clear night, whereas CODIAC acquired 6–8 marks per night. For CODIAC, gains in accuracy that reduce the required time for a successful observation offset the increased installation time. The steps involved in completing observations with the four systems, along with their corresponding data-processing strategies, are shown in Fig. 3. During an observation sequence, CODIAC and QDaedalus provide real-time fault detection, while VESTA and TSACS runs tend to only reveal faults in the collected data after the observation has been completed. TSACS, which has a minimalist interface, provides a basic pass/fail field quality check at the

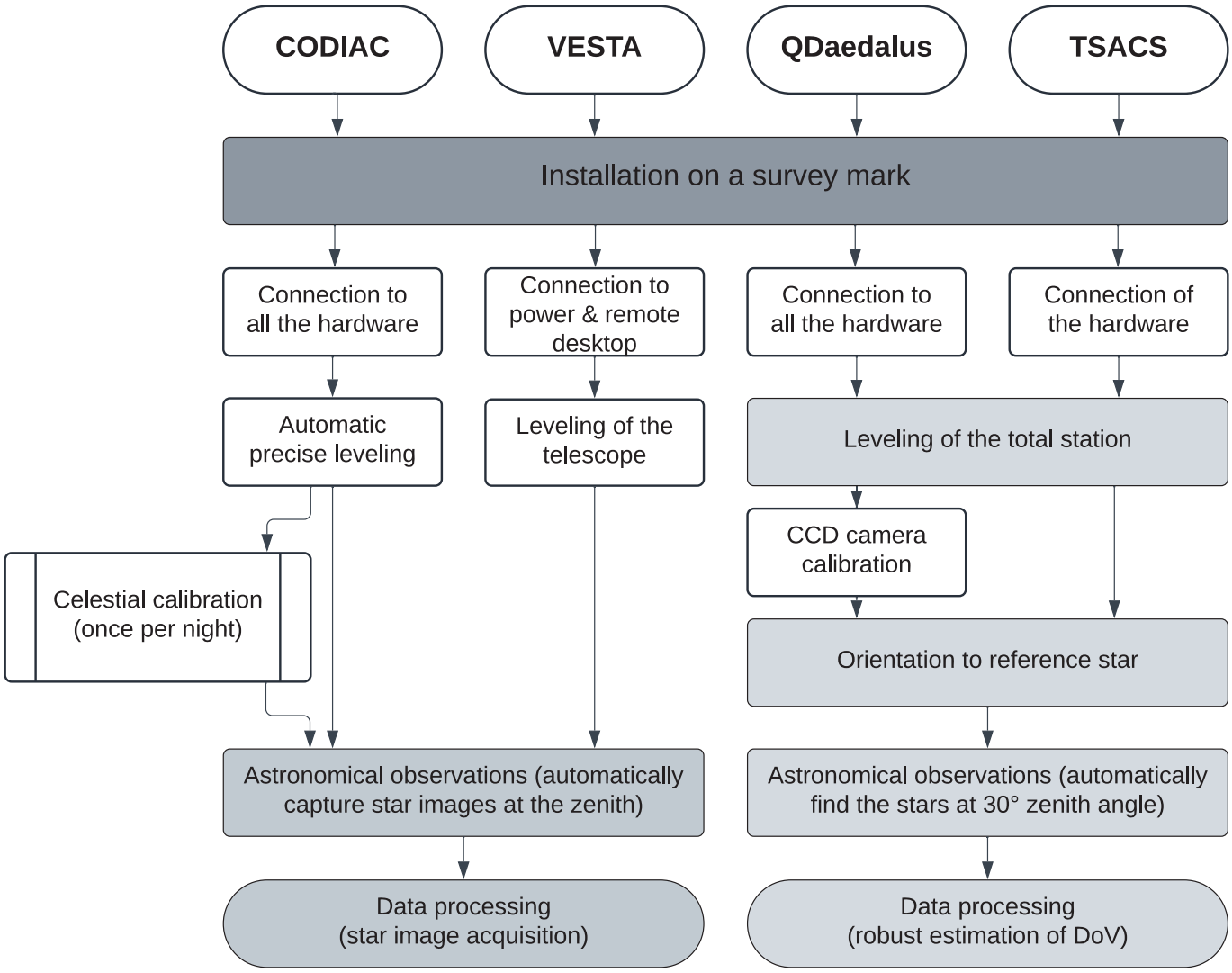

Fig. 3. The steps involved in completing observations with CODIAC, VESTA, QDaedalus and TSACS.

end of its observing sequence, ensuring a minimum number of stars are detected and that the files are correctly formatted.

2.3. Data processing

All four astrogeodetic systems have software packages that process the collected data through an automatic processing chain. In astronomical observations, the unknown parameters to be determined are the astronomical coordinates (Λ, Φ), which can be calculated as the mathematical relation of the two space vectors $x_{topo}(t)$ and $x_{ITRS}(t)$ (e.g. [22,46]):

$$x_{topo}(t) = T(\Lambda, \Phi)x_{ITRS}(t) \quad (1)$$

Here, t denotes the time of observation, while $x_{topo}(t)$ represents the star vector in the local topocentric cartesian system, $x_{ITRS}(t)$ denotes the star vector in the International Terrestrial Reference System (ITRS). The matrix $T(\Lambda, \Phi)$ defines the transformation from the ITRS to the local topocentric cartesian system.

At this data processing stage, zenith cameras and total station–based systems follow different approaches. Zenith cameras acquire sky images and extract the stars from these images in batch, whereas total station–based systems observe by selecting individual bright target stars during the measurement process. Consequently, zenith cameras require a longer data processing stage to determine astronomical coordinates. This is because in addition to having to perform many more centroiding operations per image. The distribution of these centroids must be matched to known patterns in the catalog to determine the image center's right ascesion and declination. A step that includes precise astrometric corrections for effects like proper motion, parallax, and aberration. The processing of zenith camera data is then followed by timing, tilt and polar motion corrections to determine the astronomical coordinates of the instrument [13]. By contrast, since the star coordinates are known a priori from the catalog, the data processing stage for total station–based systems involves less processing per image and primarily involves (i) centroid determination, (ii) correcting the observations for instrumental and atmospheric effects, (iii) applying precise timing and orientation parameters, and (iv) deriving the astronomical coordinates directly from the measured star positions.

2.4. Anomalous refraction

Anomalous refraction refers to irregular or asymmetrical deviations in the apparent direction of celestial objects, caused by localized variations in atmospheric conditions such as horizontal temperature, pressure, or humidity gradients. These deviations differ from the standard, radially symmetric model of atmospheric refraction. Anomalous refraction is a major concern in astrogeodetic observations, as it represents the most significant source of error. Its effect is minimal near the

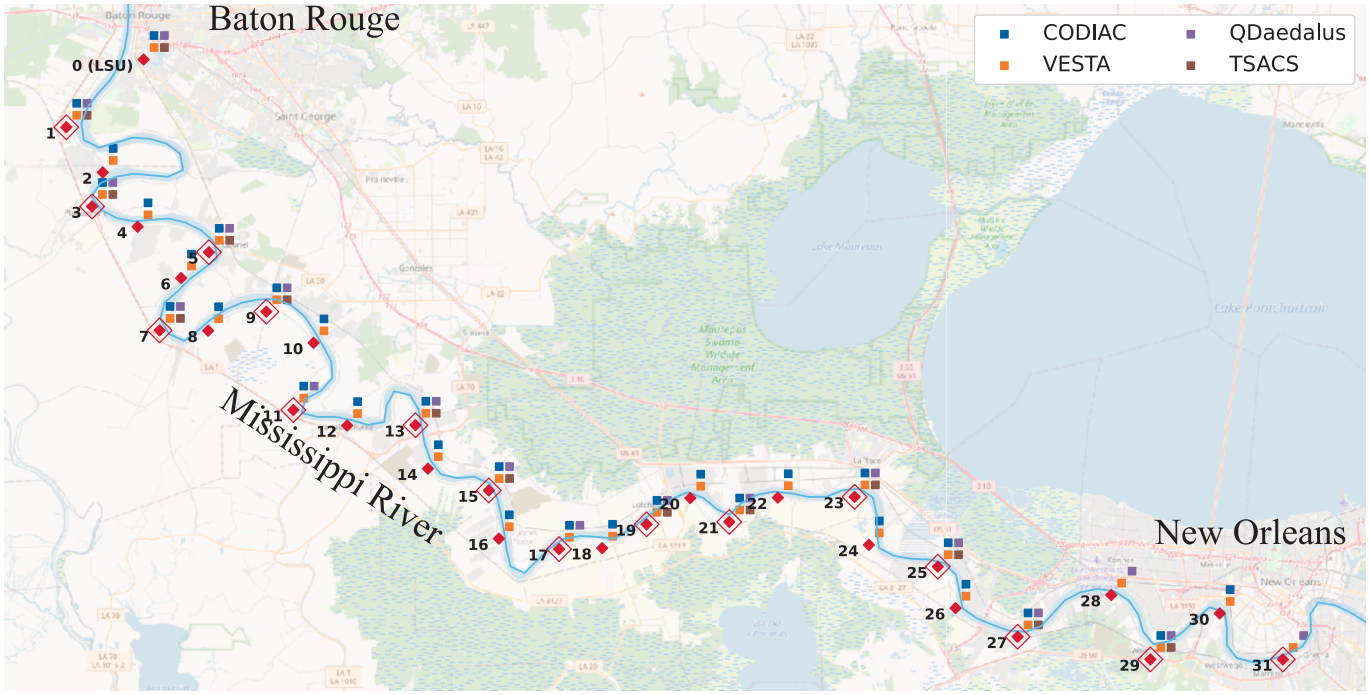

Fig. 4. Locations of astrogeodetic observations conducted using CODIAC, VESTA, QDaedalus, and TSACS along the Mississippi River, between Baton Rouge and New Orleans. Mark locations are indicated by a red diamond, while primary marks are highlighted by an enclosing outline.

zenith, but it can still result in DoV biases on the order of a few hundredths or even tenths of an arcsecond. Therefore, compared to zenith cameras, total station-based systems are more strongly affected by anomalous refraction. While reducing the zenith angle can minimize the impact of this effect, it also reduces the number of available stars. Thus, the trade-off between star visibility and refraction effects is

Table 2
Measured geodetic coordinates (in ITRF2020) and the North-South (ξ) and East-West (η) components of aggregated deflections of the vertical (DoV) for CODIAC, VESTA, QDaedalus, and TSACS.

	Geodetic Coordinates		CODIAC		VESTA		QDaedalus		TSACS	
Site	φ [°]	λ [°]	ξ [″]	η [″]	ξ [″]	η [″]	ξ [″]	η [″]	ξ [″]	η [″]
0*	30.412609	–91.181591	–0.41	–1.18	–0.28	–1.05	–0.47	–1.21	–0.63	–1.00
1	30.356123	–91.255963	0.35	–1.27	0.07	–1.06	0.10	–1.18	0.05	–0.49
2	30.318408	–91.220830	1.00	–1.00	0.67	–1.05	–	–	–	–
3*	30.289987	–91.231169	1.43	–0.93	1.60	–0.42	1.35	–1.05	1.57	–0.64
4	30.273011	–91.187349	1.67	–1.27	1.58	–1.22	–	–	–	–
5	30.251719	–91.118773	2.12	–1.36	1.87	–1.15	2.22	–1.34	1.78	–0.90
6	30.230168	–91.145497	2.43	–1.35	2.42	–1.23	–	–	–	–
7	30.186437	–91.166172	3.08	–1.09	3.24	–0.94	3.17	–1.28	2.95	–0.87
8	30.186190	–91.119480	3.06	–1.16	2.71	–1.24	–	–	–	–
9	30.202034	–91.063462	2.78	–1.33	2.67	–1.48	2.21	–1.61	2.69	–1.82
10	30.176049	–91.018047	2.67	–1.07	2.45	–0.99	–	–	–	–
11	30.119826	–91.037499	3.95	–0.90	3.83	–0.99	3.66	–1.11	–	–
12	30.106866	–90.985674	4.28	–1.07	4.06	–1.21	–	–	–	–
13*	30.107153	–90.920011	3.92	–1.36	3.79	–1.33	3.76	–1.46	3.90	–1.01
14	30.070767	–90.908022	4.42	–1.49	4.35	–1.37	–	–	–	–
15	30.052510	–90.849433	4.51	–1.39	4.17	–1.46	4.34	–1.34	4.25	–1.10
16	30.012154	–90.839710	4.55	–1.01	4.39	–0.92	–	–	–	–
17*	30.003379	–90.781818	4.68	–1.11	4.60	–1.19	4.65	–1.22	–	–
18	30.004253	–90.740341	4.80	–1.27	4.71	–1.23	–	–	–	–
19*	30.026079	–90.695482	4.29	–1.44	4.16	–1.52	4.36	–1.71	4.23	–1.84
20	30.046112	–90.655546	4.19	–1.30	3.88	–1.08	–	–	–	–
21	30.026154	–90.618048	4.29	–0.98	3.92	–0.67	4.32	–1.05	3.80	–1.04
22	30.046507	–90.571300	3.98	–0.82	4.07	–1.05	–	–	–	–
23	30.047153	–90.497479	3.93	–0.90	3.66	–0.97	3.88	–1.19	3.75	–0.62
24	30.006922	–90.483724	4.21	–0.76	3.89	–1.03	–	–	–	–
25	29.988706	–90.417392	4.27	–0.79	4.34	–1.05	4.38	–0.64	4.21	–0.66
26	29.953980	–90.400318	4.76	–0.57	5.03	–0.77	–	–	–	–
27	29.929943	–90.340601	5.00	–0.62	4.95	–0.36	4.89	–0.62	4.73	–0.40
28	29.964934	–90.250484	–	–	4.44	–0.21	4.70	–0.50	–	–
29	29.910983	–90.212871	4.86	–0.28	4.77	–0.13	4.89	0.11	4.83	0.13
30	29.949516	–90.146069	4.93	–0.25	4.40	–0.25	–	–	–	–
31	29.910970	–90.085397	–	–	5.18	0.03	5.03	0.21	–	–

*: Eccentric benchmarks were used. The geodetic coordinates provided are for CODIAC.

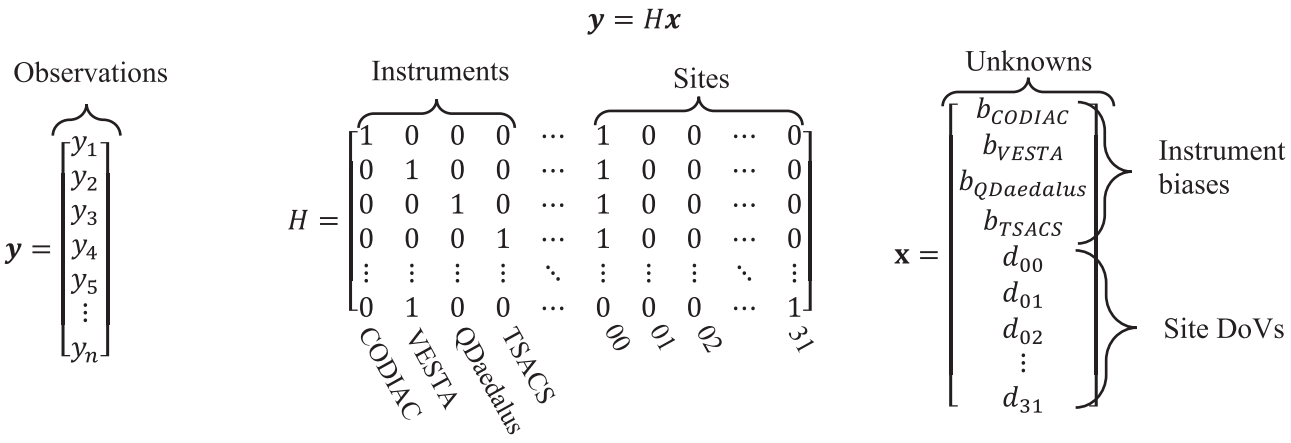

conventionally balanced at a zenith angle of 30 degrees.

3. Survey design

The astrogeodetic geoid profile was established with 32 sites spanning approximately 190 km along the Mississippi River between Baton Rouge and New Orleans. The CODIAC, VESTA, QDaedalus, and TSACS systems were used to obtain astronomical coordinates for this profile. To derive the DoV from astronomical coordinates, all sites in the survey were positioned using network-based real-time kinematic (RTK) GNSS with LSU's Center for Geoinformatics Network (C4GNET) reference station network. DoV data were collected using these four systems on 14 primary sites to enable a direct comparison of the instruments. Additionally, the VESTA was used in conjunction with one of the systems on 18 secondary intermediate sites to densify the profile for subsequent geoid determinations. The systems used at each benchmark are shown in Fig. 4.

The characteristics and constraints of each instrument influences the site selections. While the CODIAC is currently the most precise astrogeodetic system (better than $\pm$ 0.05 arcseconds, 1σ), an operator cannot use it on sloped surfaces or at locations inaccessible by commercial vehicles. Therefore, the benchmark site selections prioritized the requirements for CODIAC operations. However, five site observations used eccentric points to accommodate possible simultaneous operations with the other three tripod-mounted systems: sites 0 (LSU), 3, 13, 17, and 19. We selected these eccentric benchmarks to be within 100 m of other benchmarks at the site so that the DoV would be practically identical between these adjacent stations. The observation timeline was affected by the delayed delivery of the CODIAC system from Switzerland, which arrived one week later than expected. VESTA and QDaedalus personnel were trained on the CODIAC operation to accommodate its adjusted observation schedule due to its late transit through US customs.

4. Data collection

Our team conducted QDaedalus observations at 17 benchmarks over four nights from April 12 to 15, 2024, and we observed the LSU test site on April 18, 2024. We also performed TSACS observations at 16 of 17 planned sites over the same four nights. However, partial cloud cover and issues with missing video frames resulted in data from two sites being dropped. As TSACS and its operator were only available for ten days, these observations could not be repeated. We carried out CODIAC observations at 30 benchmarks over eight nights from April 23 to May 1, 2024. After recalibrating, we executed most of the VESTA observations from mid-May to early June 2024, except for the LSU test site, which we observed on February 3, 2025. We deployed VESTA at all 32 marks along the profile. Consequently, we used multiple instruments at the same sites on different nights. The collected DoV data from the four astrogeodetic systems, along with their geodetic coordinates, are provided in Table 2.

5. DoV estimation and instrument bias analysis

Our dataset consists of 193 discrete DoV estimates across four instruments and 32 sites. When aggregated by instrument and site, this dataset may be reduced to 93 unique site-instrument pairs. This rich dataset may be used to assess the biases and error variances of each instrument used in the campaign. To compare the performance of the systems, we performed two analyses to simultaneously estimate the site DoV and instrument biases. Of the two approaches used, the first used aggregated, unweighted DoV observed at each site. The second used more granular individual observation series returned by each instrument, with multiple observations per instrument per site. The latter case is more useful for estimating instrument uncertainties, while the former is more suited for instrument biases.

$$D_{ij} = D_i + B_j + \epsilon_j \tag{2}$$

D_{ij}: Observed deflections of the vertical (DoV)
D_i: True deflection of the vertical (DoV) at site i.
B_j: Bias for instrument j.
ϵ_j: Random error.

Then, we set up the observation equation in matrix form using a dummy matrix. The observation equation for least squares is given by:

$$\boldsymbol{y} = H\boldsymbol{x} \tag{3}$$

Solving Equation (3) provides both the instrument biases ($\widehat{\boldsymbol{b}}$) and the best estimates of the DoV in each direction ($\widehat{\boldsymbol{d}}$). This solution is tuned using the weight matrix W, a diagonal matrix with elements w_{ii} that nominally correspond to the inverse variance of each observation. This operation may be performed independently for each DoV vector component.

$$\begin{bmatrix} \widehat{\boldsymbol{b}} \\ \widehat{\boldsymbol{d}} \end{bmatrix} = (H^T W H)^{-1} H^T W \boldsymbol{y} \tag{4}$$

Equations (2)–(4) provide a general outline for performing these estimates. However, as described, the H matrix is rank-deficient, and the solution must be somehow constrained to solve for the biases and deflections simultaneously.

Table 3
Least-squares bias and precision estimates for observations aggregated by site and instrument.

Instrument	Number of sites	N-S (ξ) bias	ξ session uncertainty	E-W (η) bias	η session uncertainty
CODIAC	30	Fixed to zero	0.039″*	Fixed to zero	0.082″*
VESTA	32	–0.134″ ± 0.032″	0.17″	–0.029″ ± 0.039″	0.17″
QDaedalus	18	–0.085″ ± 0.043″	0.17″	–0.061″ ± 0.053″	0.16″
TSACS	14	–0.167″ ± 0.047″	0.15″	+0.184″ ± 0.058″	0.31″

*Based on repeat observations within a session

5.1. Approach 1: Site-Aggregated deflections

The first of these estimates was performed with aggregated deflections (one data point per instrument and site) and minimal weight assumptions. The bias column in the H matrix and the corresponding parameter vector entry for CODIAC was removed; thus, the bias for CODIAC was constrained to zero. This approach keeps the system of equations full-rank without the need for constraint equations or Lagrange multipliers. CODIAC was chosen as the zero reference because it is known to be nearly an order of magnitude more precise than its counterparts. This choice does not imply that we consider CODIAC to be the most accurate system a priori, as the design of this study does not compare the deflections of the vertical to an independent, non-astronomical standard, such as GNSS leveling or an astrogravimetric prediction. The choice of datum in a rank-deficient system is arbitrary and we believe interpretation is easiest when the zero point is the instrument with the highest repeatability and the longest track record. However, considering CODIAC's known precision advantage, this estimate was performed with a simple weighting scheme, where elements in W corresponding to CODIAC were given a value of 10 and the remaining instruments were given a value of 1. The relative weighting given to CODIAC is based on the high number of stars used per observation relative to the other three instruments, historical repeatability of CODIAC observations, and internal scatter observed in this study. This simplifies the problem to a straightforward least squares estimation, the results of which are shown in Table 3 and visualized in Fig. 5.

5.2. Approach 2: error-weighted, unaggregated observation solutions

The second analysis was performed with more granular unaggregated observations provided by each contributing research group. In

Table 4
Instrumental bias and precision estimates for each instrument based on least-squares analysis of unaggregated individual observation series.

Instruments	Number of sites	N-S (ξ) bias	ξ variability	E-W (η) bias	η variability
CODIAC	30	+0.091″ ± 0.027″	0.05″	–0.021″ ± 0.031″	0.06″
VESTA	32	–0.053″ ± 0.027″	0.08″	–0.013″ ± 0.031″	0.09″
QDaedalus	18	+0.019″ ± 0.032″	0.14″	–0.103″ ± 0.036″	0.11″
TSACS	14	–0.057″ ± 0.035″	0.09″	+0.137″ ± 0.039″	0.20″

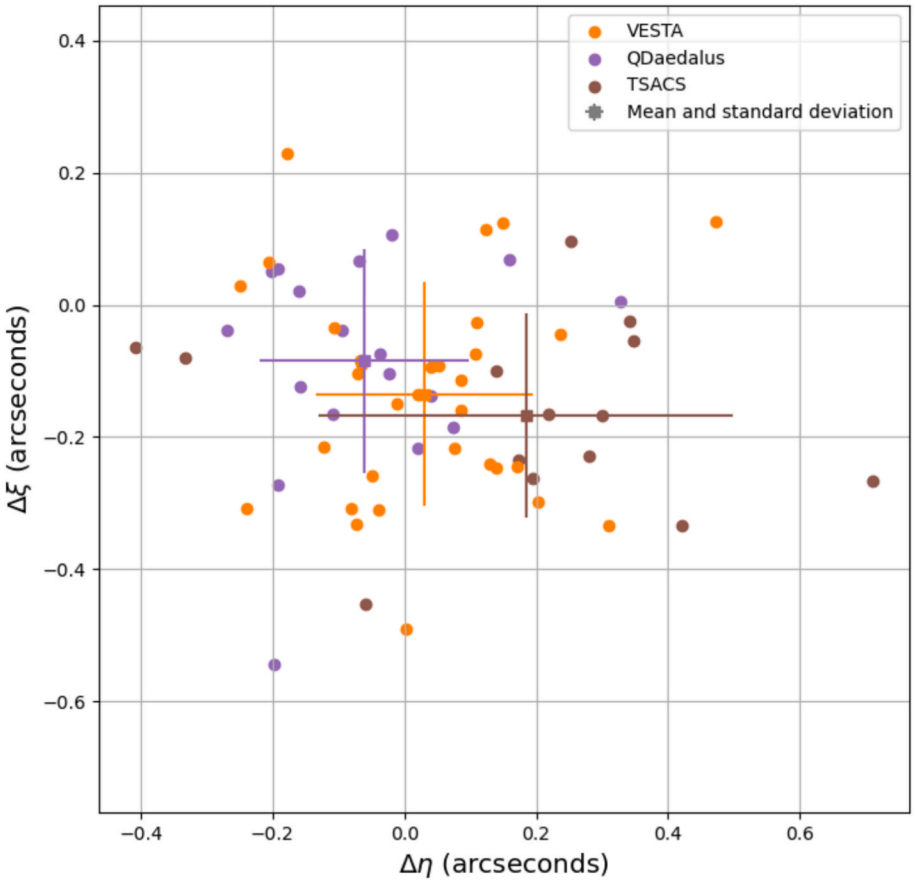

Fig. 5. Residual deflections of the vertical (Δξ and Δη) for observations aggregated by site and instrument according to a least-squares analysis centered on CODIAC.

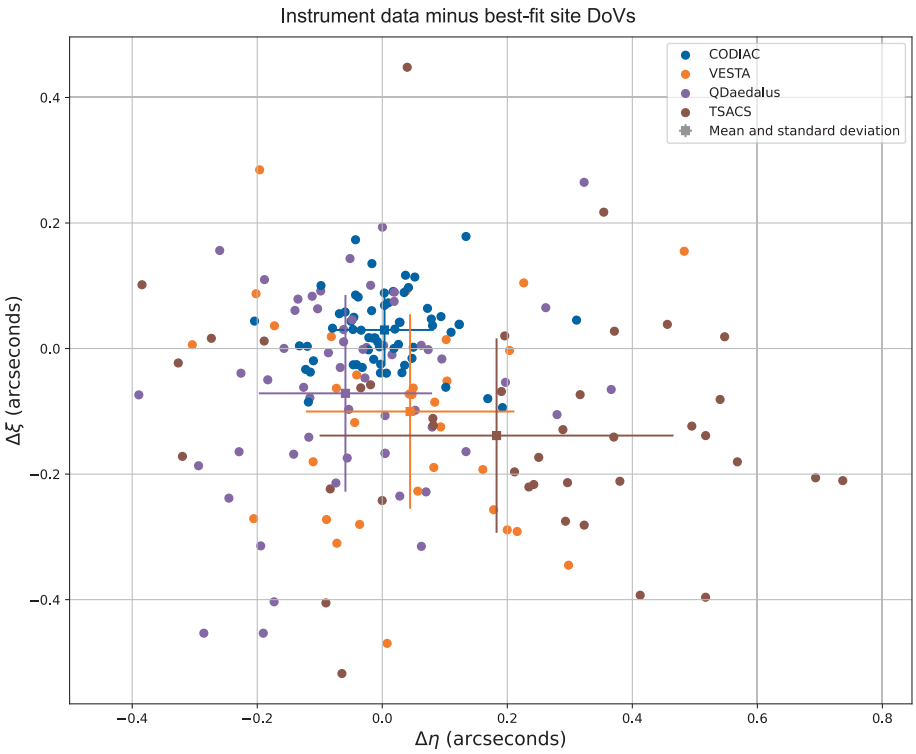

Fig. 6. Residual unaggregated deflections of the vertical (Δξ and Δη) for each instrument after subtracting the best-fit site deflections.

this instance, the estimated variances of the errors were used to weight these values in a more robust least-squares setup [47]. The weight matrix W is a diagonal matrix with elements $w_{ii} = \frac{1}{\sigma_i^2}$, where each error variance σ_i^2 corresponds to the reported error for each observation based on the residuals of individual star observations and known error characteristics for each instrument. The results of this analysis are reported in Table 4 and visualized in Figs. 6 and 7.

In contrast with the previous method, all four biases were estimated rather than fixing the CODIAC bias to zero. To address the rank deficiency we used a Lagrange multiplier scheme that imposes a constraint on the normal equations setting the observation-weighted sum of the biases to zero. This adds a row and column to the normal matrix, where each of the corresponding cells equals the sum of the *a priori* observational weights for each instrument. An extra row is added to the normal vector and filled with a zero, thus constraining the error-weighted sum of the biases to zero. This approach may be compared with the pseudo-observation approach of Koo and Clare [48] and the Lagrange multiplier technique demonstrated by Wessel [49].

6. Discussion

6.1. Field performance and operational trade-offs

The systems that participated in this survey sit at distinct corners of the trilemma regarding speed, accuracy, and deployability. The system specifications in Table 1 show that, while CODIAC sits well above its counterparts in terms of speed and accuracy, its weight detracts from its overall operational and logistical efficacy. By contrast, TSACS has the best operational performance since it consists only of a total station and lightweight third-party electronics, and once started, requires zero user intervention during the observation sequence. However, its precision could be improved. Nonetheless, its ease of use means TSACS could one day see wide use by institutions with a Leica TS60 robotic total station and appropriate GeoCOM licenses. QDaedalus has a similar level of portability, notwithstanding the laptop used for data collection, but handling the cable between the CCD camera, total station, and interface box makes it tedious to use at night. The observer cannot leave the site even for a few seconds. By contrast, TSACS can be left completely unattended during a 15-minute observation because star selection and observation scheduling are entirely automated and software-imposed rotation limits prevent cable wrapping. Like TSACS, VESTA has a similar feature in that it requires zero user intervention. Another challenge with QDaedalus is its reliance on a FireWire Type A card with an ExpressCard adapter, requiring the use of an older laptop that supports ExpressCard slots. A significant improvement to QDaedalus would be replacing the FireWire connection with a USB interface, allowing for compatibility with modern laptops and improving overall ease of use. VESTA offers precision slightly better than the total station-based systems. As a tripod-mounted system, it is lightweight and versatile compared to CODIAC. However, we found that the Lippmann tiltmeters used by both CODIAC and VESTA were sensitive to vibrations in industrial settings, such as the vicinity of oil refineries and shipping lanes, making them difficult to operate in the field.

6.2. Evaluation of instrument performance in DoV measurements

Two different estimation approaches were applied to analyze the DoV across instruments, and the findings, presented in Tables 3 and 4 and Figs. 5–7, provide insight into the performance of the four evaluated systems—CODIAC, TSACS, QDaedalus, and VESTA—for determining DoV.

The results in Table 3 and Fig. 5 show that VESTA, QDaedalus, and TSACS exhibit a bias of approximately 0.1 arcseconds to the south relative to CODIAC, which was fixed to zero. Similarly, TSACS exhibits a significant bias of nearly 0.2 arcseconds to the east relative to the other instruments. The “uncertainty” columns in this table are based on the root mean square of these observations against the mean of the entire solution. For CODIAC, this was estimated using the standard deviation of repeated observations aggregated across all sites. For the remaining sites, this was estimated using the standard deviation of the residuals of the least-squares solution (including the bias correction). These

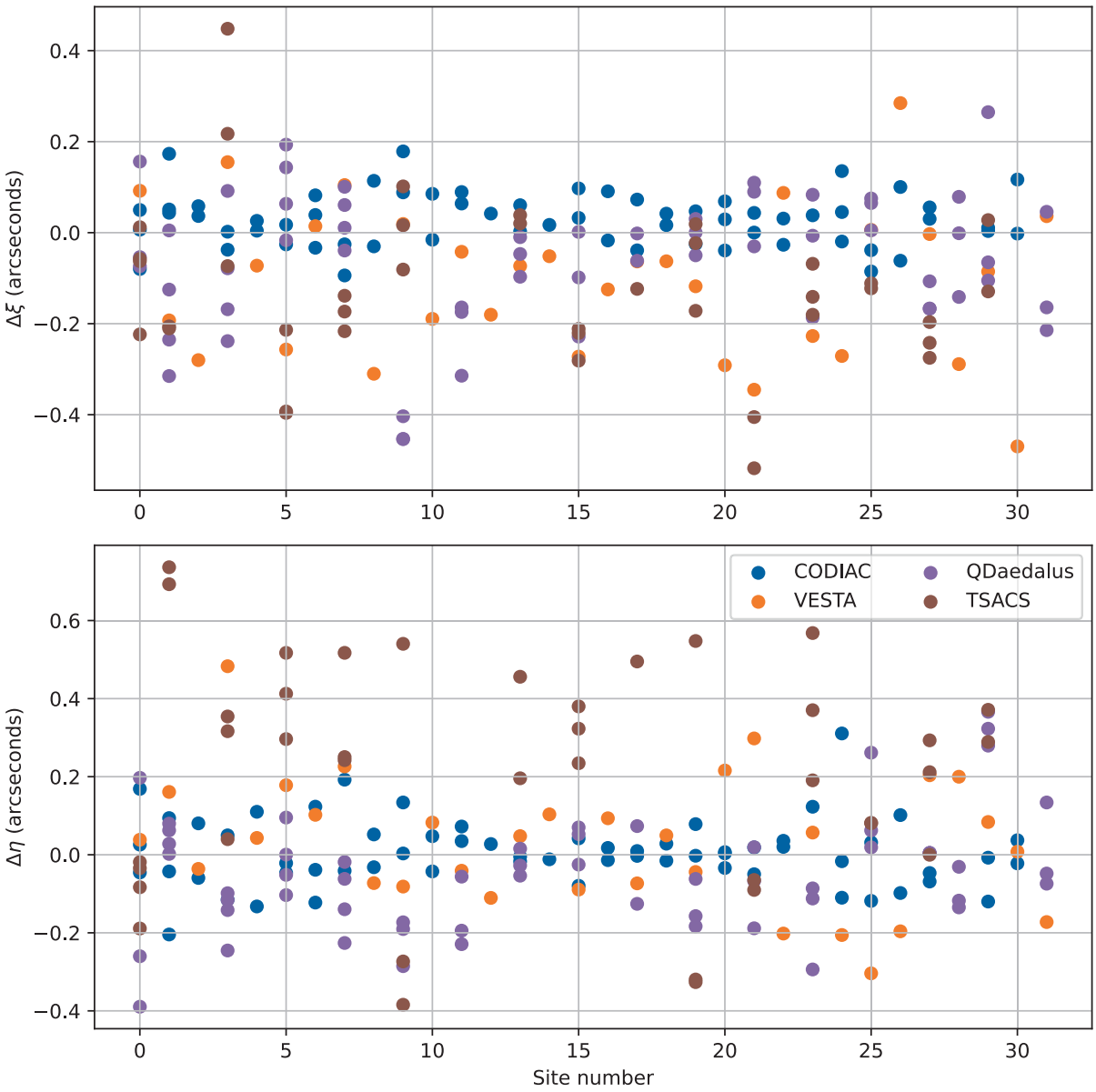

Fig. 7. Residual unaggregated deflections of the vertical (Δξ and Δη) across sites for each instrument after subtracting the best-fit site deflections.

uncertainties are less than 0.17 arcseconds, except with TSACS, which shows unexpectedly high variability in the east–west direction. As shown in Table 4 and Figs. 6 and 7, the bias solution indicates that CODIAC is about 0.1 arcseconds to the north of the other three instruments, while TSACS is approximately 0.2 arcseconds to the east, exhibiting abnormally high variability of more than 0.2 arcseconds in the east–west direction compared to its relatively stable 0.1 arcsecond residuals in the north–south direction.

After evaluating these results, CODIAC exhibited an apparent north bias, but still demonstrated the highest precision in practical site DoV measurements (20 min. observations in each benchmark, total of 30 marks), achieving an internal consistency close to its advertised ± 0.05 arcseconds within the observation sessions. This aligns with its previous performance in simultaneous parallel measurements [22,23]. CODIAC is a robust system for high-precision applications, although its north bias should be accounted for in post-processing adjustments. The relatively stable nature of the repeated observations further reinforces its reliability. VESTA and QDaedalus demonstrated moderate biases and variabilities, with both systems appearing to be systematically biased by approximately −0.1 arcseconds relative to CODIAC in the N-S direction. However, no significant biases were detected in the E-W direction for these two systems, indicating their capability to provide consistent measurements in that plane. Despite their moderate bias, VESTA and QDaedalus remain viable options for DoV determination, particularly in applications where N-S bias corrections can be systematically incorporated. TSACS meanwhile exhibited notable eastward variability and bias, primarily due to frame discontinuities in its video stream. As TSACS estimates the timing of its measurements based on the presence of time signals in its video frames, missing frames can upset the timing solution. These inconsistencies introduced errors in the E-W direction, emphasizing the need for improved video processing techniques or hardware enhancements to mitigate frame loss.

7. Summary, conclusions, and future directions

This study provides a comparative evaluation of four advanced astrogeodetic systems: two zenith cameras—CODIAC and VESTA—and two robotic total station-based systems—QDaedalus and TSACS—deployed along a 190 km geoid profile along the Mississippi River, a vital corridor for international commerce (See Sections 3 and 4). The

results obtained from this research are unique, as this is the first time four astrogeodetic systems have been deployed together for comparison at 14 primary observation sites. Moreover, the comparison was conducted using multiple instruments at different sites along the profile, rather than through repeated observations at a single site as in previous studies (See Sections 1 and 2). The findings highlight the operational challenges and technical trade-offs associated with each system in practical field applications. The overall survey, conducted at 32 sites, underscores additional operational challenges of designing an astrogeodetic profile in a busy commercial corridor.

The results demonstrate that CODIAC achieves the highest precision, with an uncertainty in the range of 0.05 arcseconds, making it the preferred choice for high-accuracy geodetic applications. VESTA, QDaedalus, and TSACS exhibited higher measurement uncertainty, with an expected accuracy of approximately 0.15 arcseconds when using 45-minute occupations (See Section 5). While this level of accuracy is suitable for many geodetic applications, users should be aware of the individual system characteristics and potential systematic biases when integrating these measurements into broader geodetic models. The unique strengths of each system provide valuable options for different observational and logistical constraints (See Section 6).

While this work focuses solely on the instrument performance and lessons learned in survey design, these findings contribute directly to geoid validation efforts, particularly in Louisiana, where rapid subsidence and data gaps complicate geoid modeling. The results will support refining the GEOID2022 model and future geodetic field campaigns to improve orthometric height determination. This work has already had an impact on NGS products. Hardy et al. [50] presented a poster, and Hardy [51] delivered a public webinar on the geodetic implications of the data we collected. Future research should focus on refining data processing methodologies, addressing systematic biases, and enhancing instrumentation for improved determinations of the DoV. Expanding similar comparative studies to diverse geographic and environmental conditions will further contribute to optimizing astrogeodetic methodologies for geoid modeling and broader geodetic applications.

Funding

This research was funded by the Graduate Women in Science (GWIS) fellowship and by the Geospatial Center for the Arctic and Pacific (GCAP) using Federal funds under Geospatial Modeling Grant NA23NOS4000333, "NSRS Modernization and Geodetic Workforce Development in the Arctic and Pacific Region," from NOAA National Geodetic Survey (NGS), U.S. Department of Commerce. The statements, findings, conclusions, and recommendations are those of the authors and do not necessarily reflect the views of NGS or the U.S. Department of Commerce.

CRediT authorship contribution statement

Müge Albayrak: Writing – review & editing, Writing – original draft, Visualization, Validation, Supervision, Resources, Project administration, Methodology, Investigation, Funding acquisition, Formal analysis, Data curation, Conceptualization. **Ryan A. Hardy:** Writing – review & editing, Writing – original draft, Visualization, Validation, Supervision, Software, Resources, Project administration, Methodology, Investigation, Funding acquisition, Formal analysis, Data curation, Conceptualization. **Benjamin A. Fernandez:** Writing – review & editing, Writing – original draft, Validation, Supervision, Methodology, Investigation, Formal analysis, Data curation. **Jon Cliburn:** Writing – review & editing, Formal analysis, Data curation. **Aline P. Baeriswyl:** Writing – review & editing, Data curation. **Daniel Willi:** Writing – review & editing, Validation, Software, Resources, Funding acquisition, Data curation. **Sébastien Guillaume:** Writing – review & editing, Software, Resources, Funding acquisition, Data curation.

Declaration of competing interest

The authors declare that they have no known competing financial interests or personal relationships that could have appeared to influence the work reported in this paper.

Acknowledgments

The authors thank the Graduate Women in Science (GWIS) Fellowship Committee and the Geospatial Center for the Arctic and Pacific (GCAP) for supporting this research. The Center for Geoinformatics (C4G) at Louisiana State University (LSU) provided significant support for this project. Special thanks to Dr. George Voyiadjis, Dr. Clifford Mugnier and J. Anthony Cavell for providing access to LSU facilities, as well as for the VESTA, relative gravimeter, GNSS equipment, Leica TS60 total station, and various fieldwork supplies. Additionally, we are grateful for the contributions and support of Oregon State University (OSU), NOAA's National Geodetic Survey (NGS), the Swiss Federal Office of Topography swisstopo, and the School of Management and Engineering Vaud (HEIG-VD), along with their staff. We also thank our internal reviewers, Dr. Christopher E. Parrish at OSU, and Dr. Derek Van Westrum and Dr. Andria Bilich at NGS, for their diligent reviews and insightful comments.

Appendix A

Table A1
Statistical summary of DoV data collected with CODIAC before (2021) and after (2025) the CMOS camera upgrade at the Zimmerwald Observatory. The 2021 CODIAC data represent three days of observations, while the 2025 CMOS-upgrade data correspond to one night of observations. The standard deviations are comparable, although the percentage of outliers is slightly higher in the post-upgrade data, likely due to the shorter observation period.

Observed Year	DoV Components	Mean [″]	SD [″]	Total Number of Series	Outliers (N)	Outliers (%)
2021	N-S [ξ]	7.83	0.060	107	16	15.00 %
	E-W [η]	3.95	0.151	107	6	5.60 %
2025	N-S [ξ]	7.88	0.067	29	5	17.20 %

Data availability

The original contributions presented in the study are included in the article; further inquiries can be directed to the corresponding author.

References

[1] A.R. Robbins, Deviation of the vertical, Emp. Surv. Rev. 11 (1951) 28–36, https://doi.org/10.1179/sre.1951.11.79.28.

[2] W.A. Heiskanen, H. Moritz, Physical Geodesy, Inst. Phys. Geod., Tech. Univ. Graz, Austria, 1984.

[3] M. Albayrak, U. Marti, D. Willi, S. Guillaume, R.A. Hardy, Precise geoid determination in the eastern swiss alps using geodetic astronomy and GNSS/leveling methods, Sensors 24 (2024) 7072, https://doi.org/10.3390/s24217072.

[4] S. Guillaume, Determination of a Precise Gravity Field for the CLIC Feasibility Studies, Ph.D. Thesis, ETH Zurich, Switzerland, 2015, doi: 10.3929/ethz-a-010549038.

[5] S. Guillaume, J. Clerc, C. Leyder, J. Ray, M. Kistler, Contribution of the image-assisted theodolite system QDaedalus to geodetic static and dynamic deformation monitoring, 3rd Joint Int. Symp. Deform. Monitoring (JISDM), 2016, http://www.fig.net/resources/proceedings/2016/2016_03_jisdm_pdf/nonreviewed/JISDM_2016_submission_66.pdf.

[6] A. Zarinš, A. Rubans, G. Silabriedis, Digital zenith camera of the University of Latvia, Geod. Cartogr. 42 (2016) 129–135, https://doi.org/10.3846/20296991.2016.1268434.

[7] L. Tian, J. Guo, Y. Han, X. Lu, W. Liu, Z. Wang, B. Wang, Z. Yin, H. Wang, Digital zenith telescope prototype of China, Chin. Sci. Bull. 59 (2014) 1978–1983, https://doi.org/10.1007/s11434-014-0256-z.

[8] C. Shi, C. Zhang, L. Du, J. Li, K. Ye, W. Zhang, C. Chen, C. Li, L. Ma, H. Lin, K. Mi, Automatic astronomical survey method based on video measurement robot, J. Surv. Eng. 146 (2020) 04020002, https://doi.org/10.1061/(ASCE)SU.1943-5428.0000300.

[9] J.C. Hughes, J. Dunlap, S. Johnson, C.G. Olson, R. Siegert, J.H. Song, W. Wangler, Development of a digital zenith camera for precision determination of gravitational deflection of the vertical, AGU Fall Meet. (2019). https://agu.confex.com/agu/fm19/meetingapp.cgi/Paper/516824.

[10] R.A. Hardy, K. Fancher, K. Ahlgren, B. Erickson, C. Geoghegan, S. Breidenbach, S. Hilla, Geodetic astronomy with an imaging robotic total station, AGU Fall Meet. (2020). https://agu.confex.com/agu/fm20/meetingapp.cgi/Paper/674689.

[11] M.M. Murzabekov, V.F. Fateev, D.I. Pleshakov, Results of astronomical leveling on the Moscow attraction using a zenith camera, Geodezia i Kartografia 84 (2023) 2–9 (in Russian), doi: 10.22389/0016-7126-2023-1002-12-2-9.

[12] A. Călin, P. Dumitru, O. Bădescu, A. Savu, New astro-geodetic measurements for geoid modeling, Rom. Astron. J. 33 (2024) 183–198.

[13] C. Hirt, B. Bürki, A. Somieski, G. Seeber, Modern determination of vertical deflections using digital zenith cameras, J. Surv. Eng. 136 (2010) 1–12, https://doi.org/10.1061/(ASCE)SU.1943-5428.0000009.

[14] A.E. Somieski, Astrogeodetic Geoid and Isostatic Considerations in the North Aegean Sea, Greece, Ph.D. Thesis, ETH Zurich, Switzerland, 2008, doi: 10.3929/ethz-a-005710420.

[15] C. Hirt, Entwicklung und Erprobung Eines Digitalen Zenitkamerasystems für Die Hochpräzise Lotabweichungsbestimmung, Ph.D. Thesis, Univ. Hannover, Germany, 2004 (in German).

[16] C. Hirt, G. Seeber, Accuracy analysis of vertical deflection data observed with the Hannover Digital Zenith Camera System TZK2-D, J. Geodesy 82 (2008) 347–356, https://doi.org/10.1007/s00190-007-0184-7.

[17] M. Hauk, C. Hirt, C. Ackermann, Experiences with the QDaedalus system for astrogeodetic determination of deflections of the vertical, Surv. Rev. 49 (2017) 294–301, https://doi.org/10.1080/00396265.2016.1171960.

[18] C. Voigt, Astrogeodatische Lotabweichungen zur Validierung von Schwerefeldmodellen, Ph.D. Thesis, Leibniz Univ. Hannover, Germany, 2013 (in German).

[19] M. Albayrak, C. Hirt, S. Guillaume, K. Halicioglu, M.T. Özlüdemir, C.K. Shum, Quality assessment of global gravity models in coastal zones: a case study using astrogeodetic vertical deflections in Istanbul, Turkey, Stud. Geophys. Geod. 64 (2020) 306–329, https://doi.org/10.1007/s11200-019-0591-2.

[20] M. Albayrak, K. Halicioglu, M.T. Özlüdemir, B. Basoglu, R. Deniz, A.R.B. Tyler, M. M. Aref, The use of the automated digital zenith camera system in Istanbul for the determination of astrogeodetic vertical deflection, Bull. Geod. Sci. 25 (2019) 1–23, https://doi.org/10.1590/s1982-21702019000400025.

[21] R.A. Hardy, K. Fancher, B. Erickson, S. Breidenbach, K. Ahlgren, D. van Westrum, C. Geoghegan, S. Hilla, K. Jordan, Performance assessment of the Total Station Astrogeodetic Control System (TSACS), AGU Fall Meet. (2021). https://agu.confex.com/agu/fm21/meetingapp.cgi/Paper/813173.

[22] M. Albayrak, D. Willi, S. Guillaume, Field comparison of the total station-based QDaedalus and the zenith telescope-based CODIAC astrogeodetic systems for measurements of the deflection of the vertical, Surv. Rev. 55 (2023) 247–259, https://doi.org/10.1080/00396265.2022.2054108.

[23] I. Varna, D. Willi, S. Guillaume, M. Albayrak, A. Zarins, M. Ozen, Comparative measurements of astrogeodetic deflection of the vertical by latvian and swiss digital zenith cameras, Remote Sens. 15 (2023) 2166, https://doi.org/10.3390/rs15082166.

[24] G.G. Bennett, J.G. Freislich, Field astronomy for surveyors, N.S.W. Univ. Press, Kensington, Australia, 1979, 251 pp.

[25] U. Marti, Comparison of high precision geoid models in Switzerland, in: P. Tregoning, C. Rizos (Eds.), Dynamic Planet, IAG Symp., Springer, Berlin/Heidelberg, 2007, pp. 271–278.

[26] K. Morozova, R. Jäger, A. Zarins, J. Balodis, I. Varna, G. Silabriedis, Evaluation of quasi-geoid model based on astrogeodetic measurements: case of Latvia, J. Appl. Geod. 15 (2021) 319–327, https://doi.org/10.1515/jag-2021-0030.

[27] D.A. Smith, S.A. Holmes, X. Li, S. Guillaume, Y.M. Wang, B. Bürki, D.R. Roman, T. M. Damiani, Confirming regional 1 cm differential geoid accuracy from airborne gravimetry: the geoid slope validation survey of 2011, J. Geod. 87 (2013) 885–907, https://doi.org/10.1007/s00190-013-0653-0.

[28] Y.M. Wang, C. Becker, G. Mader, D. Martin, X. Li, T. Jiang, S. Breidenbach, C. Geoghegan, D. Winester, S. Guillaume, B. Bürki, The geoid slope validation survey 2014 and GRAV-D airborne gravity enhanced geoid comparison results in Iowa, J. Geod. 91 (2017) 1261–1276, https://doi.org/10.1007/s00190-017-1022-1.

[29] D. van Westrum, K. Ahlgren, C. Hirt, S. Guillaume, A geoid slope validation survey (2017) in the rugged terrain of Colorado, USA, J. Geod. 95 (2021) 9, https://doi.org/10.1007/s00190-020-01463-8.

[30] C. Hirt, S. Claessens, T. Fecher, M. Kuhn, R. Pail, M. Rexer, New ultrahigh-resolution picture of Earth's gravity field, Geophys. Res. Lett. 40 (2013) 4279–4283, https://doi.org/10.1002/grl.50838.

[31] N.K. Pavlis, S.A. Holmes, S.C. Kenyon, J.K. Factor, The development and evaluation of the Earth Gravitational Model 2008 (EGM2008), J. Geophys. Res. Solid Earth 117 (2012) B04406, https://doi.org/10.1029/2011JB008916.

[32] K. Ahlgren, GeMS Validation Survey, NGS webinar series (2022), https://www.ngs.noaa.gov/web/science_edu/webinar_series/gems-validation-survey.shtml (accessed 10 Jan 2024).

[33] U.S. Department of Transportation, Bureau of Transportation Statistics, Freight Facts and Figures, Washington, DC, 2020.

[34] National Geodetic Survey, Blueprint for 2022, Part 2: Geopotential Coordinates, NOAA Tech. Rep. NOS NGS 64 (2017), https://www.ngs.noaa.gov/PUBS_LIB/NOAA_TR_NOS_NGS_0064.pdf.

[35] C. Fitzpatrick, K.L. Jankowski, D. Reed, 2023 Coastal Master Plan: Determining Subsidence Rates for Use in Predictive Modeling, Coastal Prot. Restor. Auth., Baton Rouge, LA, 2020, https://coastal.la.gov/wp-content/uploads/2021/03/Subsidence-Rates_Mar2021.pdf.

[36] L. Nadolinets, E. Levin, D. Akhmedov, Surveying instruments and technology, CRC Press, 2017.

[37] G. Tóth, L. Völgyesi, Data processing of QDaedalus measurements, Geosci. Eng. 5 (2017) 147–164.

[38] B.T. Erickson, Astrogeodetic Investigations of the Gravity Field in Central Ohio with a Robotic Total Station, Master Thesis, Ohio State Univ., Columbus, USA, 2022, http://rave.ohiolink.edu/etdc/view?acc_num=osu1650580386093472.

[39] B. Bürki, ICARUS, Astro-geodetic on-line observation system–User manual V.05, Geod. Geodyn. Lab, ETH Zurich, Switzerland, 2005.

[40] A. Zarinš, A. Rubans, G. Silabriedis, Performance analysis of Latvian zenith camera, Geodesy Cartogr. 44 (2018) 1–5, https://doi.org/10.3846/gac.2018.876.

[41] N. Zacharias, C.T. Finch, T.M. Girard, A. Henden, J.L. Bartlett, D.G. Monet, M. I. Zacharias, The fourth US naval observatory CCD astrograph catalogue (UCAC4), Astron. J. 145 (2013) 44. https://iopscience.iop.org/article/10.1088/0004-6256/145/2/44.

[42] T. Prusti, J.H.J. de Bruijne, A.G.A. Brown, A. Vallenari, C. Babusiaux, C.A.L. Bailer-Jones, U. Bastian, M. Biermann, D.W. Evans, L. Eyer, F. Jansen, S. Zschocke, The Gaia mission, Astron. Astrophys. 595 (2016) A1, https://doi.org/10.1051/0004-6361/201629272.

[43] R. Wielen, H. Schwan, C. Dettbarn, H. Lenhardt, H. Jahreiss, R. Jährling, Sixth catalogue of fundamental stars (FK6), Part I, Veroeff. Astron. Rechen-Inst. Heidelberg 35 (1999) 1.

[44] M.A. Perryman, L. Lindegren, J. Kovalevsky, E. Hoeg, U. Bastian, P.L. Bernacca, C. S. Petersen, The HIPPARCOS catalogue, Astron. Astrophys. 323 (1997) L49–L52.

[45] C. Hirt, T. Kahlmann, Hochpräzise Neigungsmessung mit dem elektronischen Pendelneigungssensor HRTM, Z. Vermessungswesen 129 (2004) 266–276, in German.

[46] S. Guillaume, B. Bürki, S. Griffet, H.M. Durand, QDaedalus: Augmentation of total stations by CCD sensor for automated contactless high-precision metrology, Proc. FIG Working Week, Rome, Italy, 6–10 May 2012, http://www.fig.net/resources/proceedings/fig_proceedings/fig2012/papers/ts09i/TS09I_guillaume_buerki_et_al_6002.pdf.

[47] S.R. Searle, An overview of variance component estimation, Metrika 42 (1995) 215–230, https://doi.org/10.1007/BF01894301.

[48] A. Koo, J.F. Clare, On the equivalence of generalized least-squares approaches to the evaluation of measurement comparisons, Metrologia 49 (2012) 340, https://doi.org/10.1088/0026-1394/49/3/340.

[49] P. Wessel, Tools for analyzing intersecting tracks: the x2sys package, Comput. Geosci. 36 (2010) 348–354.

[50] R.A. Hardy, M. Albayrak, B. Fernandez, J. Cliburn, D. Willi, S. Guillaume, Geoid Validation with Astronomical Leveling along the Mississippi River, AGU Fall Meet. https://agu.confex.com/agu/agu24/meetingapp.cgi/Paper/1568503.

[51] R.A. Hardy, The Southern Louisiana Astrogeodetic Survey: Assessing the Performance of GEOID2022 along the Mississippi River, NGS webinar series (2025), https://www.ngs.noaa.gov/web/science_edu/webinar_series/astrogeodetic-survey.shtml (accessed 28 Feb 2025).